ADVANCED MATERIALS
www.advmat.de

A Universal Ternary Solvent System of Surface Passivator Enables Perovskite Solar Cells with Efficiency Exceeding 26%

*Qiang Zhang, Hao Huang, Yingying Yang, Min Wang, Shujie Qu, Zhineng Lan, Tongtong Jiang, Zhiwei Wang, Shuxian Du, Yi Lu, Yi Suo, Peng Cui, and Meicheng Li**

Surface passivation is a vital approach to improve the photovoltaic performance of perovskite solar cells (PSCs), in which the passivator solvent is an inevitable but easy-ignored factor on passivation effects. Herein, a universal ternary solvent system of surface passivators is proposed through comprehensively considering the solubility and selective perovskite dissolution of the solvent to maximize the passivation effect. Tetrahydrothiophene 1-oxide (THTO) is selected as the passivation promoter by comparing the binding energy with perovskite and the ability to distort the perovskite lattice among various aprotic polar solvent molecules, which can facilitate the passivator's reaction with perovskite and achieve sufficient passivation on perovskite surface. Besides, chlorobenzene (CB) is used as the diluting agent to minimize the amount of isopropanol (IPA), inhibiting the additional solvent-induced defects. As a result, the planar PSCs achieve a power conversion efficiency (PCE) of 26.05%, (certificated 25.66%). Besides, the unencapsulated devices exhibit enhanced stability, which can maintain 95.23% and 95.68% of their initial PCE after 2000 h of storage in ambient air and 800 h of light-soaking in N_2-glovebox. Moreover, this ternary solvent system also exhibits a well applicability and reliability in different passivator such as PEAI, BAI, and so on.

1. Introduction

Perovskite solar cells (PSCs) have been considered as the most promising new generation photovoltaic technology, due to distinguish advantages, such as simple preparation, high efficiency, and so on.[1,2] In the past decade, various strategies have been proposed to improve the power conversion efficiency (PCE) of PSCs, such as bulk doping, energy level modulation, charge transport layer optimization and defect passivation, improving the latest certified PCE to be 26.7%.[1–6] Among these strategies, defect passivation is considered as the most efficient method to lift the PCE, because there exists a large number of defects in perovskite films, especially their surface.[7,8] Hence, it is supposed to be a feasible approach to improve the photovoltaic performance of PSCs that developing and optimizing the surface passivation technology.

Designing and selecting the suitable material to serve as the passivator is the key part to achieve an effective passivation for improving the PSCs' efficiency. In the past years, various materials have been proposed, including Lewis bases, Lewis acids, and organic ammonium salts, etc.[9,10] Among them, organic ammonium salts represented by phenethyl ammonium iodide (PEAI) have been wildly used.[11–13] In 2019, You et al. first utilized the PEAI to passivate perovskite surface, achieving a certificated PCE of 23.32%, the highest value at that time.[14] Since then, passivating perovskite surface using PEAI and its derivatives has been intensively reported, and even became a normal technology to fabricate high-efficiency PSCs.[13] As more and deeper insight into the surface passivating using PEAI and its derivatives, researchers begin to pay attention to the solvent and its influence on PSCs during the passivation process since the solvent is inevitable in a spin-coating method, the most common method to introduce passivator on the surface.[15–17] Isopropanol (IPA), acts as a popular solvent, and has been used in most studies of PSCs surface treatment, since it is excellent in dissolving passivated materials. However, formamidinium iodide (FAI), itself with the amidinium functional group, is also soluble in IPA which can cause additional defects on the surface, particularly formamidine iodide (FAI)-based films. As a result, poor reproducibility, device instability, and other issues are prevalent when using it as the solvent of passivator to passivate perovskite film surface.[17,18] To address this issue, diluting IPA using non-polar solvents was reported. Xiao et al. dissolved the passivating material GABr in a mixed solvent of IPA and toluene to alleviate the destructive effect of IPA on perovskite, achieving an improvement in the PSCs' photovoltaic performance.[17]

Q. Zhang, H. Huang, Y. Yang, M. Wang, S. Qu, Z. Lan, T. Jiang, Z. Wang, S. Du, Y. Lu, Y. Suo, P. Cui, M. Li
State Key Laboratory of Alternate Electrical Power System with Renewable Energy Sources
School of New Energy
North China Electric Power University
Beijing 102206, China
E-mail: mcli@ncepu.edu.cn

The ORCID identification number(s) for the author(s) of this article can be found under https://doi.org/10.1002/adma.202410390

DOI: 10.1002/adma.202410390

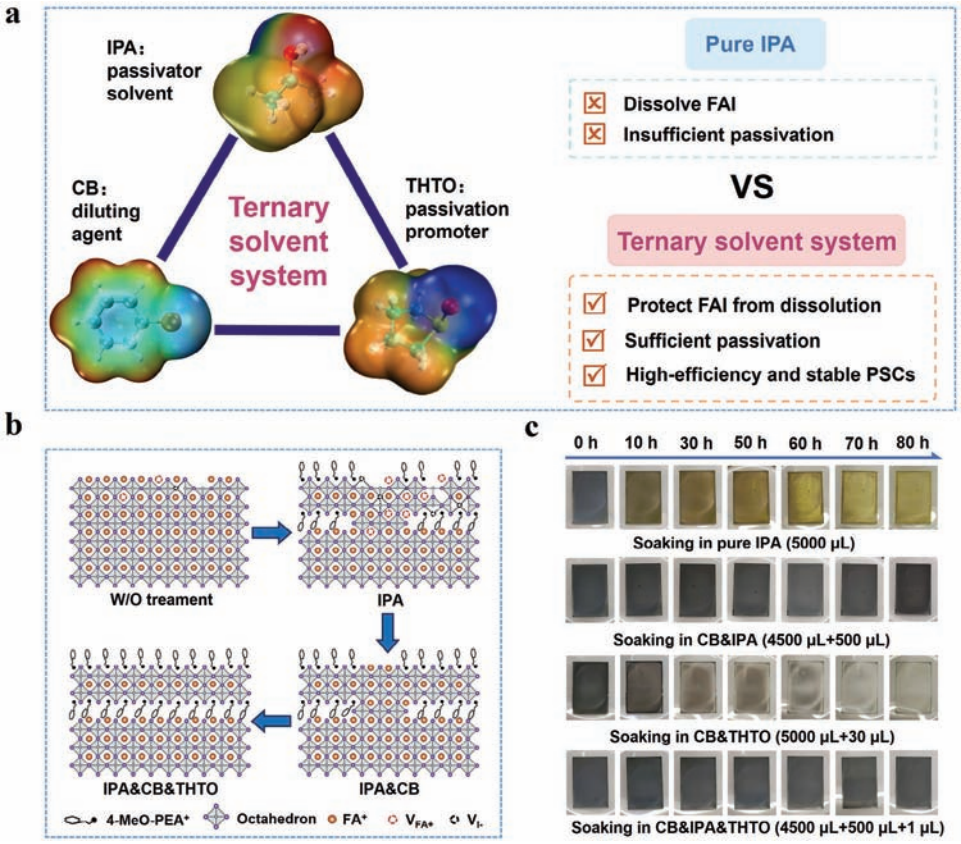

Figure 1. Design principle of ternary solvent system. a) Schematic diagram of ternary solvent system. b) Schematic diagram of passivation using 4-MeO-PEAI dissolved in different solvents. c) The morphology evolution of perovskite films soaked in different solvents.

Besides, it was reported that the organic ammonium salts can induce 2D perovskite in the surface, achieving the defects passivation and stability enhancement.[19] Promoting the penetration of organic ammonium salts and the formation of 2D perovskite can improve the passivation effects. Ye et al. introduced the N, N-dimethylformamide (DMF) into the IPA solvent, which can achieve a global incorporation of butylammonium cations at both surface and bulk grain boundaries since DMF can dissolve the PbI_2 and perovskite inorganic frameworks, enabling strain-free perovskite films with simultaneously reduced defect density.[15] From the above analysis, it is found that the solvent of passivation materials exhibited a significant influence on the passivation effects, in which finely controlling the capability of solvent in dissolving passivator and its selective dissolution on perovskite component is necessary to maximize the potential of surface passivation on improving photovoltaic performance of PSCs.

In this work, a ternary solvent system of 4-methoxyphenethylammonium iodide (4-MeO-PEAI) was proposed to synergistically protect the perovskite surface and promote the penetration of 4-MeO-PEAI, enabling the high-quality perovskite surface with reduced defects and enhanced 2D capping layer. In the ternary solvent system, the main component is chlorobenzene (CB), a solvent that hardly dissolves perovskite, the minimum IPA was incorporated to dissolve the 4-MeO-PEAI and the tetrahydrothiophene 1-oxide (THTO) was incorporated to promote the penetration of 4-MeO-PEAI through softening the perovskite inorganic framework. As a result, the resulting PSCs achieved a champion PCE of 26.05% with a fill factor of 83.71% and an open circuit voltage (V_{OC}) of 1.187 V. Besides, the unencapsulated PSC can maintain 95.23% and 95.68% of its initial PCE after storing in ambient conditions for over 2000 h and light soaking in N_2-glovebox for ≈800 h.

2. Results and Discussion

In order to construct a state-of-the-art solvent system to maximize the passivation effect, we developed a ternary solvent system that consists of IPA, CB, and THTO. As shown in **Figure 1**a,b, in the ternary solvent system, the IPA is served as passivator solvent, the CB is a diluting agent as the main component, and the THTO is served as passivation promoter. As a proton polar solvent, when using the IPA as the single solvent of 4-MeO-PEAI, the IPA will inevitably destroy the perovskite surface through dissolving FAI, resulting the additional defects, especially the FA^+ vacancy.[16,17] To alleviate this perovskite destruction, we utilized CB as the diluting agent to decrease the amount of IPA at the basis of sufficient dissolution of the passivator. Besides, in view of the insufficient reaction between the passivator and the surface, we introduced THTO, an aprotic polar solvent that can soften the perovskite structure, to serve as the passivation promoter, ensuring sufficient passivation through promoting the penetration of 4-MeO-PEAI and the formation of 2D perovskite.

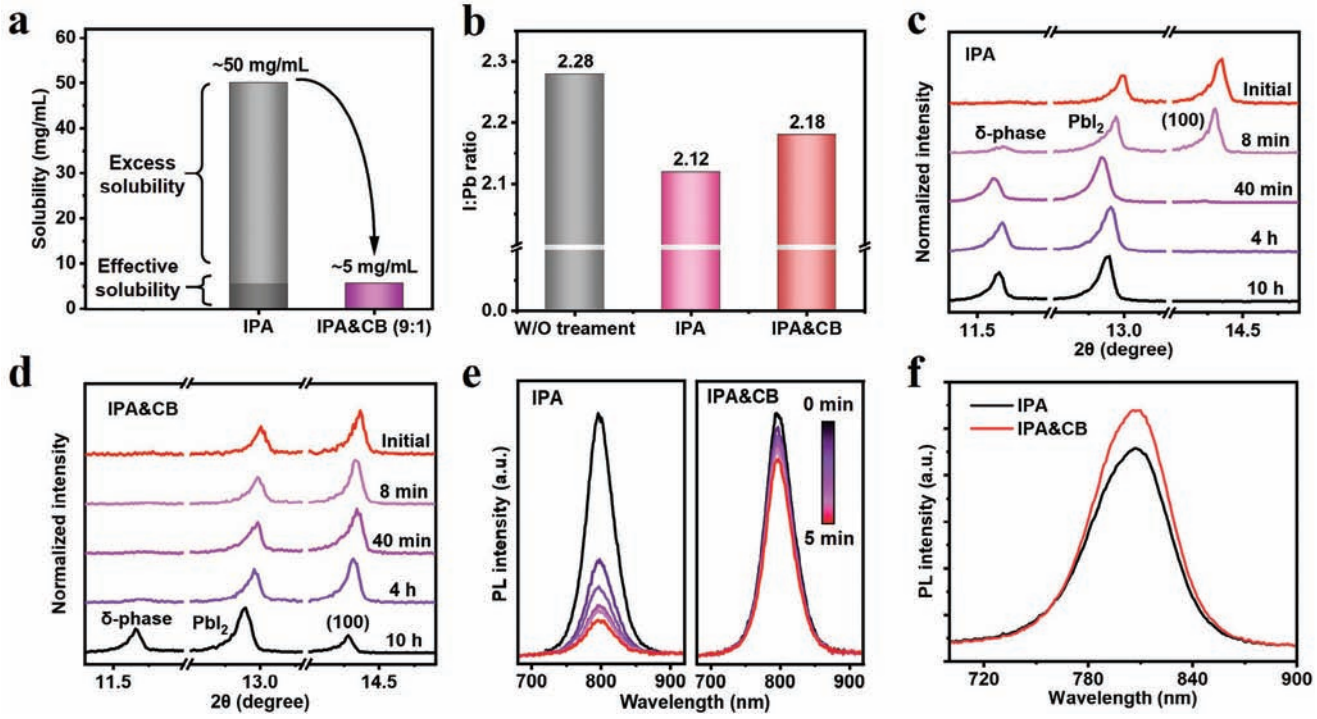

Figure 2. The protective effect of chlorobenzene on perovskite. a) The evaluated solubility of IPA and IPA&CB (1:9) mixed solvent. b) The calculated I:Pb ratios of the perovskite surface. c,d) XRD patterns of perovskite films. e) PL spectra of perovskite films after immersing into IPA and IPA&CB (1:9) solvent. f) PL spectra of perovskite films passivated by 4-MeO-PEAI in IPA and IPA&CB (1:9).

To preliminary validate the dissolution of different solvents on perovskite, the perovskite films were soaked into IPA, IPA&CB, CB&THTO, and IPA&CB&THTO at different times to observe the changes (Figure 1c). We found that the perovskite film soaked in IPA (5000 µL) gradually turned into a yellow phase, suggesting the dissolution of FA^+. This deficiency of FA^+ is prone to inducing the perovskite to form δ-phase and PbI_2. In comparison, the perovskite film soaked in the IPA&CB (500 µL+ 4500 µL) can always maintain a black color, indicating the alleviated dissolution of FA^+ from IPA. The perovskite film can be immediately dissolved after soaking into pure THTO (5000 µL), leaving the transparent FTO substrate (Figure S1, Supporting Information). To slow down this dissolution, we soaked the perovskite film in the CB&THTO (5000 µL+30 µL), and then we found that the perovskite was gradually dissolved. These results indicate that the THTO can destruct the perovskite inorganic framework and PbI_2, which is different from the IPA. When decreasing the amount of THTO on the ternary solvent system, the perovskite can maintain the black color, which provides the potential to utilize the ternary solvent system in the practical fabrication of PSCs.

We now explore the influence of diluting agent (CB) on the passivation effects. The solubility of 4-MeO-PEAI in IPA was determined to be ≈50 mg mL^{-1} (Figure S2, Supporting Information). In the normal experiment, the concentration of 4-MeO-PEAI solution is 5 mg mL^{-1}, which indicates that the excess IPA can be replaced by CB which is served as diluting agent (**Figure 2a**). To explore the influence of mixed solvent (the volume ratio of IPA:CB is 1:9) on perovskite surface, the IPA solvent and mixed solvent of IPA&CB were applied on perovskite by spin-coating, and then these films were characterized by X-ray photoelectron spectroscopy (XPS) to detect the I: Pb ratio (Figure 2b). The I: Pb ratio of perovskite film with surface clean by IPA is 2.12, which is obviously lower than that (2.28) of perovskite film without surface solvent clean. This decreased I:Pb ratio may results from the dissolved FAI by IPA.[16] After using mixed solvent to clean the surface, the I: Pb ratio of perovskite film is 2.18, indicating the diluting agent of CB can effectively alleviate the FAI dissolution. The XRD characterization was used to investigate the crystal structure changes of perovskite films that were soaked in different solvent. When the perovskite film was soaked in IPA, the δ-phase began to appear at 8 min. As the immersing time increased to 40 min, the perovskite film completely degraded into PbI_2 and δ-phase (Figure 2c),[20,21] which is consistent with the phenomenon in Figure 1c. In comparison, this perovskite degradation can be greatly slowed down in the mixed solvent, and the δ-phase only shows an obvious increment after 10 h of immersion (Figure 2d). We also monitored the photoluminescence (PL) evolution of perovskite films soaked in IPA and IPA&CB, respectively. The PL intensity of perovskite film soaked in IPA degraded to 33% of its initial value within 5 min (Figure 2e). By contrast, the films soaked in the IPA&CB showed enhanced stability, and the PL intensity can retain 85% of its initial value after 5 min-soaking. These above results confirm that IPA solvent shows a detrimental effect on perovskite film, and this detrimental effect can significantly be alleviated by introducing CB as the diluting agent, which is also reflected in the photovoltaic performance of PSCs (Figure S3 and Note S1, Supporting Information). Further

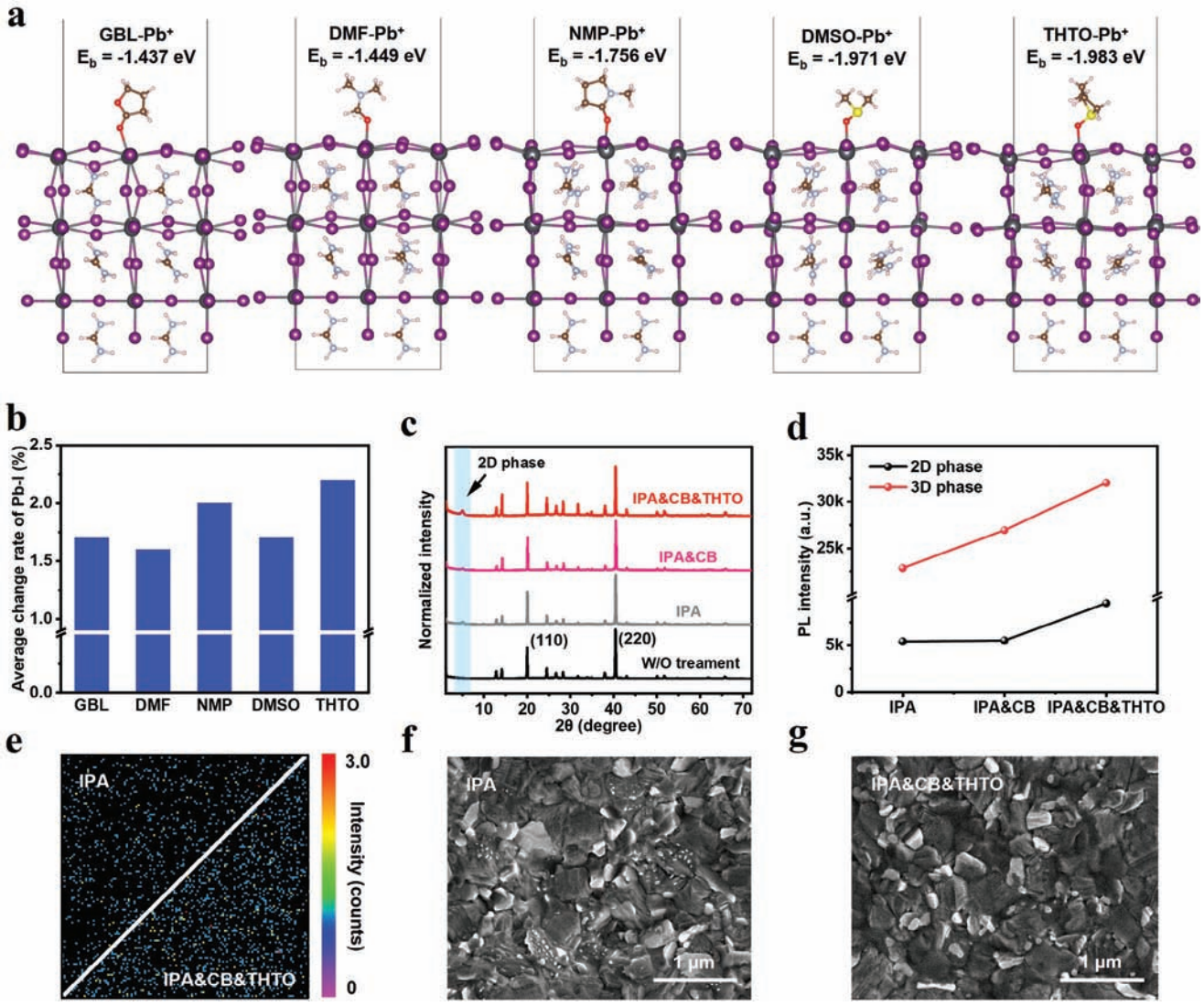

Figure 3. Effect of passivator promoter (THTO) on surface passivation. a) Adsorption model and the corresponding binding energy of different aprotic polar solvent molecules (including GBL, DMF, NMP, DMSO, THTO) with $FAPbI_3$ structure. b) The average change rate of the five Pb—I bond length around the adsorbed Pb. c) XRD spectra of the perovskite films. d) The evolution of PL intensity of 3D and 2D perovskite. e) SIMS mapping of 4-MeO-PEA^+ cation for perovskite films. f,g) Top-view SEM image of the perovskite films.

to investigate the diluting agent on the surface passivation effects, we performed PL characterization on perovskite films that were passivated by 4-MeO-PEAI solution using IPA and IPA&CB as the solvent. Compared to perovskite film passivated by 4-MeO-PEAI in IPA, the perovskite film passivated by 4-MeO-PEAI in IPA&CB shows a stronger PL intensity, indicating that the utilization of CB as diluting agent can achieve a more effective surface passivation (Figure 2f).[22] After determining the detailed utilization and effect of CB, we accordingly determined the main component of the solvent system. Then, we will explore the utilization and effect of THTO, the promoter, based on this solvent system of IPA&CB.

We now turn to discuss the passivation promoter and its function in our ternary solvent system. Before determining the materials to serve as passivation promoters, we carried out density functional theory calculation to calculate the binding energy (E_b) between perovskite with a series of aprotic polar solvents. As shown in **Figure 3**a, all the selected aprotic polar solvents can be stably adsorbed on perovskite through binding with Pb^{2+}. Among them, the E_b between THTO and perovskite is the highest. Compared to the normal perovskite lattice (Figure S4, Supporting Information), the adsorbed solvent molecular can obviously induce the lattice distortion, including the length changes of Pb—I bond and the rotation of FA^+. We calculate the length of five Pb—I bonds near the adsorbed Pb^{2+}, and then compared them with corresponding Pb—I bonds in normal perovskite lattice to obtain the average change rate of Pb—I length, a value to quantitatively evaluate the perovskite lattice distortion. The Figure 3b shows the average change rate of Pb—I length of perovskite lattice after adsorbed by different solvent molecules, and the detailed calculation information is shown in Table S1 (Supporting Information). When the perovskite lattice is adsorbed by THTO, the average

change rate of Pb-I length is the largest, which indicates that the THTO can obviously distort and soften the perovskite lattice. This large perovskite lattice distortion is supposed to be beneficial to promote the penetration of 4-MeO-PEAI and its reaction with perovskite. Hence, the THTO was determined to be the passivation promoter in our ternary solvent system.

To investigate the promoted effect of THTO on surface passivation, we first carried out X-ray diffraction to characterize perovskite film, and perovskite films passivated by 4-MeO-PEAI dissolved in different solvents. As shown in Figure 3c, surface passivation can induce the formation of 2D perovskite, which is consistent with the previous reports.[23,24] In detail, the diluting agent of CB shows a minor effect on the formation of 2D perovskite. As a comparison, the THTO that served as the passivation promotor can obviously promote the formation of 2D perovskite. The evolution of 2D phase was also validated by the measurement of grazing incidence X-ray diffraction (GIXRD) with the incident angle of 0.5° (Figure S5, Supporting Information). The perovskite films passivated by 4-MeO-PEAI in different solvents were also characterized by PL measurement (Figure S6, Supporting Information). Figure 3d exhibits the evolution of PL intensity of 3D and 2D perovskite respectively, in which we can find that although the diluting agent shows a minor effect on the formation of 2D perovskite, it can achieve a more effective passivation due to it can suppress the additional defects resulted from the destruction of IPA on perovskite. After incorporating the THTO, the PL intensity of 2D perovskite shows an obvious improvement, suggesting the increased 2D perovskite,[25,26] which is consistent with the XRD results. Notably, the PL intensity of 3D perovskite also shows a large improvement, which should result from the promoted formation of 2D perovskite on the surface. Both the results of XRD and PL measurements confirm that the THTO can function as the passivation promoter, contributing to achieving more effective surface passivation with an optimized surface energy landscape (Figure S7 and Note S2, Supporting Information). Further to validate the promoted penetration of 4-MeO-PEAI and its reaction with perovskite, the measurements of time-of-flight secondary ion mass spectrometry (TOF-SIMS) and scanning electron microscope (SEM) were carried out on perovskite passivated by 4-MeO-PEAI dissolved in IPA and IPA&CB&THTO, respectively. Figure 3e shows the 2D distribution of 4-MeO-PEA$^+$ on the perovskite surface, where the intensity of 4-MeO-PEA$^+$ on perovskite film passivated by 4-MeO-PEAI dissolved in IPA&CB&THTO is obviously higher than that on perovskite film passivated by 4-MeO-PEAI dissolved in IPA, indicating the promoted penetration of 4-MeO-PEAI. The TOF-SIMS depth profile of 4-MeO-PEA$^+$ on both perovskite films shown in Figure S8 (Supporting Information) also proves that more 4-MeO-PEA$^+$ can penetrate into the perovskite. In addition, the SEM results shown in Figure 3f,g exhibit that the perovskite film passivated by 4-MeO-PEAI dissolved in IPA&CB&THTO possesses a more compact surface with reduced residual PbI_2, this reduced PbI_2 can be also validated by the cross-sectional SEM images (Figure S9, Supporting Information), indicating the promoted reaction between 4-MeO-PEAI with perovskite.

In order to investigate the effect of ternary solvent system on the photoelectric property of perovskite film and PSCs' physical property, we carried out various measurements, including time-resolved photoluminescence (TRPL), PL mapping, electrochemical impedance spectroscopy (EIS) and so on. Before discussion, for the convenience of description, we name the perovskite film passivated by 4-MeO-PEAI dissolved in IPA and the corresponding PSCs (fluorine-doped tin oxide (FTO)/compact-titanium dioxide (c-TiO_2)/perovskite/4-MeO-PEAI/2,2′,7,7′-tetrakis [N, N-di(4-methoxyphenyl) amino]-9-9′-spirobifluorene (Spiro-OMeTAD)/Au) as a control sample, and the perovskite film passivated by 4-MeO-PEAI dissolved in ternary solvent system and the corresponding PSCs as target sample. First, we performed space-charge limited current (SCLC) measurements of electron-only devices (FTO/c-TiO_2/perovskite/phenyl-C61-butyric acid methyl ester (PCBM)/Au) to evaluate the defect density. As shown in **Figure 4a,b**, the V_{TFL} of the control device is 0.26 V, and the V_{TFL} of the target device is 0.15 V. According to the equation of $N_t = (2\epsilon\epsilon_0 V_{TFL})/(qL^2)$, the smaller V_{TFL} means the corresponding perovskite film has a lower defect density.[27,28] TRPL was carried out to characterize the carrier lifetime of perovskite film. As shown in Figure 4c and Table S2 (Supporting Information), the average carrier lifetime of target perovskite is 819.99 ns, higher than that (468.55 ns) of control film. In addition, the average carrier lifetime of perovskite film passivated with the solvent of passivator is IPA&CB is 666.75 ns (Figure S10, Supporting Information). The results of TRPL measurement demonstrate that the ternary solvent system can optimize the surface passivation effect, leading to a reduced nonradiative recombination.[29]

To evaluate the photoelectric properties of perovskite film in terms of spatial uniformity, we performed PL mapping to characterize both control and target perovskite films (Figure 4d,e). The PL intensity of target perovskite is obviously greater than that of control perovskite. Besides, the distribution of the PL intensity in the target film is more spatially uniform. The improved optoelectronic properties and spatial uniformity of perovskite film is beneficial for reducing the nonradiative carrier recombination, which can be confirmed by the EIS spectra where the target PSC exhibits a higher R_{rec} (Figure 4f) and dark J–V curves where the target PSC exhibits a smaller dark saturation current (Figure S11, Supporting Information).[30,31] In short, the ternary solvent system can synergistically inhibit the IPA-induced defects during the surface passivation and promote the penetration of 4-MeO-PEAI and its reaction with perovskite, ensuring a non-destructive and sufficient surface passivation (Figure 4g).

We fabricated planar PSCs and characterized their photovoltaic performance to investigate the influence of ternary solvent systems on PSCs' performance. Based on the relatively optimal recipe of a ternary solvent system (Figure S12, Supporting Information), the target PSCs achieve a champion PCE of 25.52% with a short current density (J_{SC}) of 26.08 mA cm^{-2}, a V_{OC} of 1.174 V and an FF of 83.36% (**Figure 5a**). As a comparison, the control PSCs only achieve a champion PCE of 24.65%, with a J_{SC} of 26.00 mA cm^{-2}, a V_{OC} of 1.161 V, and an FF of 81.69%. Figure 5b exhibits the distribution diagram of PCE for a batch of control and target PSCs, respectively, where the target PSCs possess a higher average PCE of 25.07% than that (24.37%) of control PSCs. To explore the universal effectiveness of the ternary solvent system on other passivators, we also fabricated PSCs using BAI, p-Br-PEAI, o-F-PEAI, CF_3-PEAI, and PEAI as perovskite surface passivator. No matter which passivators we use, the ternary solvent system

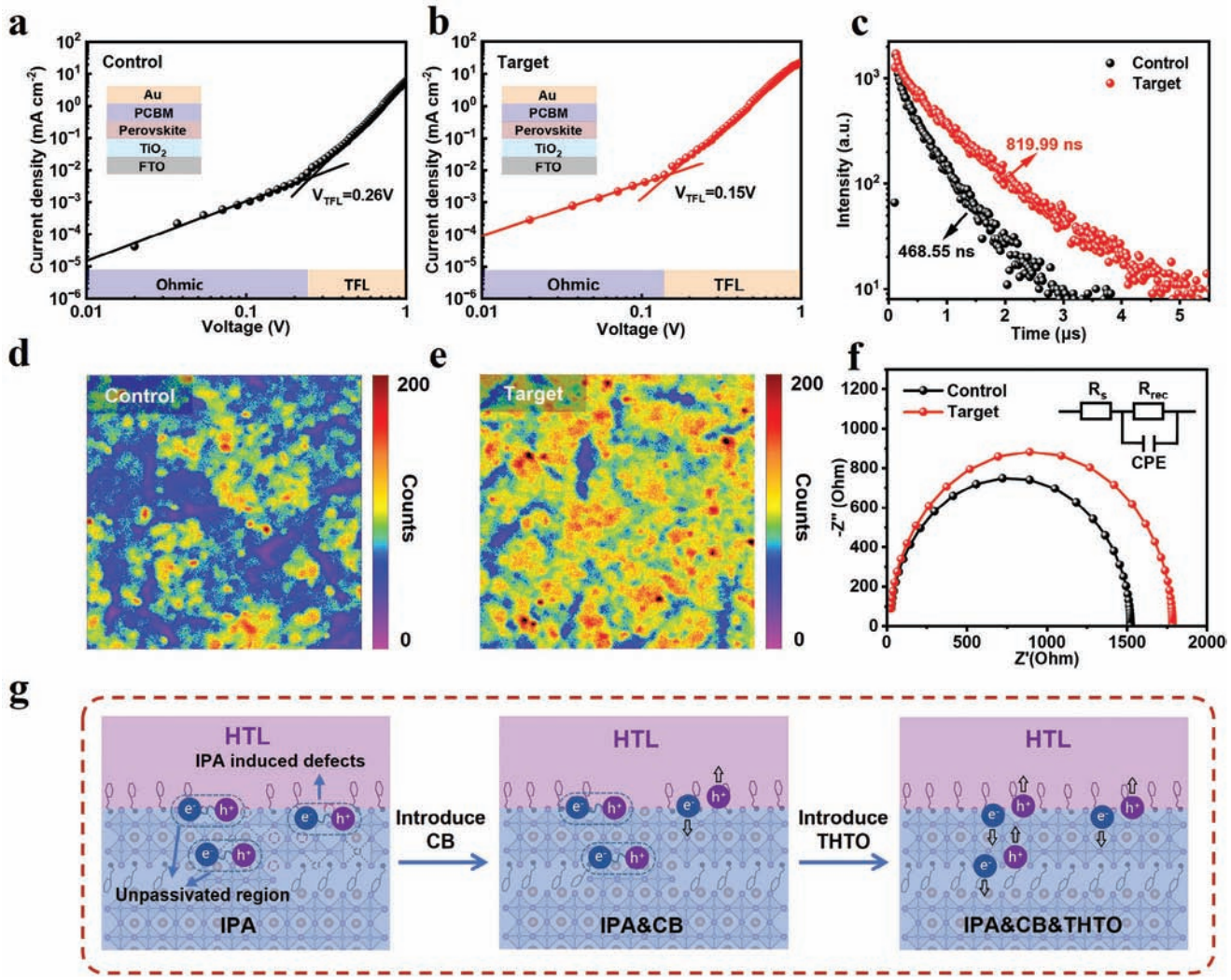

Figure 4. Passivation effects using ternary solvent system. a,b) Space charge limited current curves for electron-only devices. c) TRPL spectra of control and target perovskite films. d,e) PL mapping of control and target perovskite films. The detected size is 25 μm × 25 μm. f) Nyquist plots of control and target PSCs. Insert shows the equivalent circuit mode. g) A schematic diagram of that ternary solvent system can inhibit the IPA-induced defects and promote the penetration of passivator (4-MeO-PEAI) and its reaction with perovskite, ensuring sufficient surface passivation.

can enhance the surface reaction and optimize the surface passivation, which can be supported by reduced surface roughness and changes of surface potential. (Figures S13 and S14, Supporting Information). As displayed in Figure 5c and Figure S15 (Supporting Information), no matter what kind of passivator we use, the ternary solvent system shows a positive effect on improving the photovoltaic performance of PSCs. Among other passivators, the PSCs passivated by o-F-PEAI show highest PCE, which may result from that the o-F-PEAI can be adsorbed stronger onto the acceptor defects due to the enhanced electropositivity of -NH_3^+ terminals due to the existence of the F atom, producing a better passivation effect.[32]

In this work, if not specified, the perovskite film is fabricated by one-step spin-coating method with ether as the antisolvent, and the electron transport layer (ETL) for device is TiO_2. To demonstrate the reliable effect of ternary solvent system, we further fabricated perovskite film using two-step spin-coating method and then fabricated planar PSCs structured as FTO/Tin oxide (SnO_2)/perovskite/4-MeO-PEAI/Spiro/Au. As shown in Figure 5d, the target PSCs achieve a champion PCE of 26.05% (J_{SC} = 26.22 mA cm^{-2}, V_{OC} = 1.187 V, FF = 83.71%) with small hysteresis (Table S3, Supporting Information). In comparison, the control PSCs only obtain a champion PCE of 25.28% (J_{SC} = 26.10 mA cm^{-2}, V_{OC} = 1.174 V, FF = 82.52%). The statistic distributions of photovoltaic parameters obtained from PSCs where perovskite films fabricated by two-step method are presented in Figure 5e and Figure S16 (Supporting Information), the target PSCs show an excellent reproducibility with an improved average PCE of 25.53%. One of our best-performing PSCs has been sent to a third-independent institute of the National Institute of Metrology for certification and obtained a certificated PCE of 25.66% (Figure S17, Supporting Information), validating this reliable effect of ternary solvent system on fabricating high-efficiency PSCs. Moreover, we also fabricated inverted PSCs

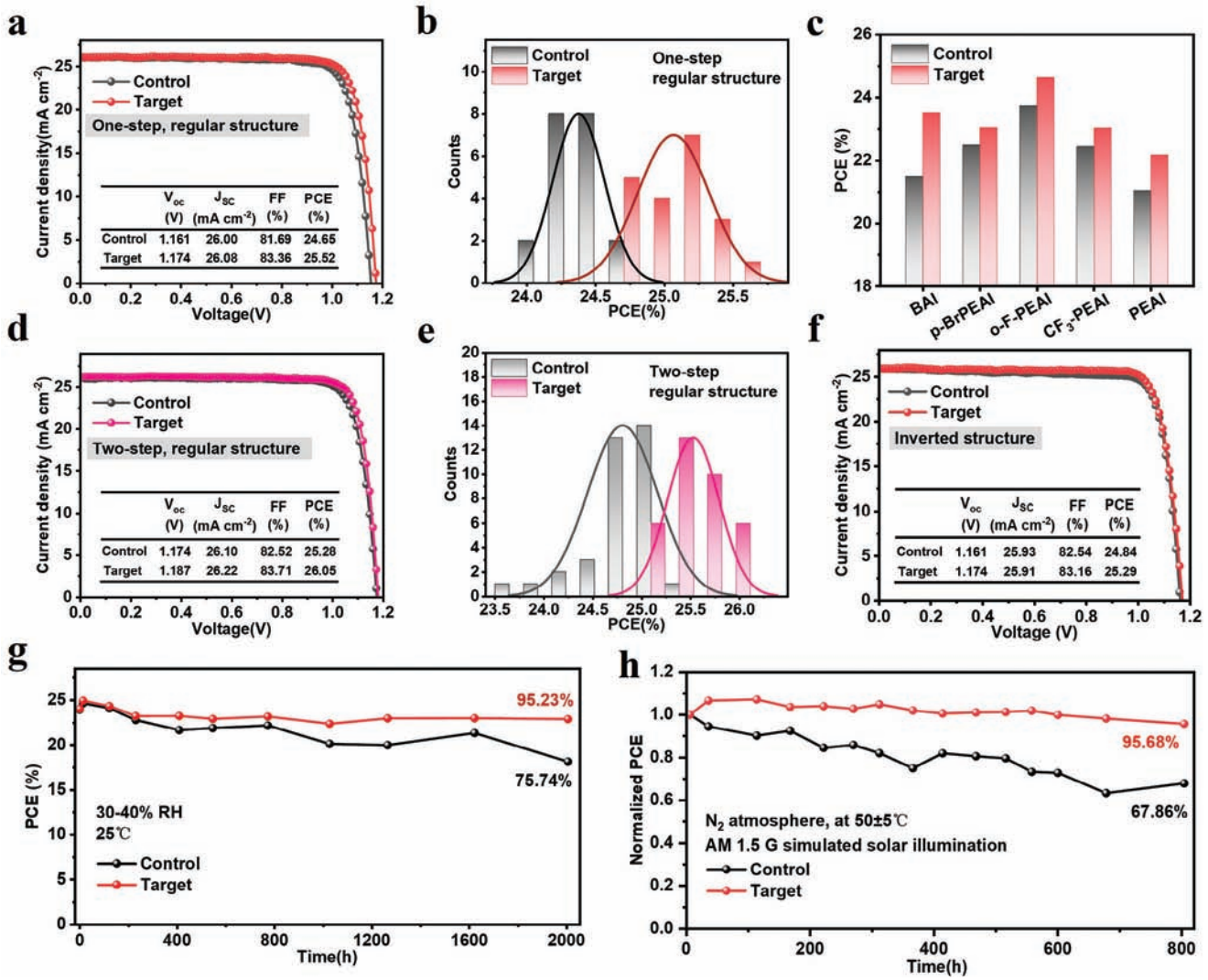

Figure 5. Photovoltaic performance and stability of PSCs where the active area is 0.08 cm^2. a) The reverse *J–V* curves of control and target PSCs where the perovskite film is fabricated by one-step method. b) PCE statistics for 20 control and target PSCs, respectively. The perovskite film is fabricated by one-step method. c) PCE comparison of PSCs using the BAI, p-BrPEAI, o-F-PEAI, CF_3-PEAI, and PEAI as the surface passivators. The perovskite film is fabricated by one-step method. d) The reverse *J–V* curves of control and target PSCs where the perovskite film is fabricated by two-step method and the ETL is SnO_2. e) Distribution histograms of PCE value among 35 control and target PSCs, respectively. The perovskite film is fabricated by two-step method and the ETL is SnO_2. f) The reverse *J–V* curves of control and target inverted PSCs, the device structure was FTO/Ni_xO/[4-(3,6-Dimethoxy-9H-carbazal-9-yl) butyl] phosphonic Acid (MeO-4PACz) /perovskite/phenylethylammonium chloride (PEACl)/ fullerene (C60)/2,9-dimethyl-4,7-diphenyl-1,10-Phenanthroline (BCP)/Ag. g) Storage stability of the unencapsulated control and target PSCs in ambient conditions. h) Light-soaking stability of control and target PSCs.

using our ternary solvent system. As shown in Figure 5f, the champion PCE of the target inverted PSCs achieve a PCE of 25.29% (J_{SC} = 25.91 mA cm^{-2}, V_{OC} = 1.174 V, FF = 83.16%), higher than that (24.84%) of control inverted PSCs. The integrated J_{SC} calculated from the external quantum efficiency (EQE) spectrum of target inverted PSCs, shown in Figure S18 (Supporting Information), yields a small variation with the J_{SC} value in Figure 5f. Besides, the target inverted PSCs also possess good reproducibility (Figure S19, Supporting Information).

After confirming the effectiveness of ternary solvent system on improving photovoltaic performance, its influence on device stability has also been explored. First, the storage stability of the unencapsulated control and target devices in an ambient condition of ≈25 °C and relatively humidity (RH) of 30–40% was monitored. As presented in Figure 5g, the target device can maintain 95.23% of its initial PCE after 2000 h storage, while the control device maintains 75.74% of its initial PCE. This enhanced storage stability was also validated by other passivators-applied devices (Figure S20, Supporting Information). The light-soaking stability with the device stored in a N_2-glovebox was also tested and the corresponding results are shown in Figure 5h. After 800 h light-soaking, the target device can maintain 95.68% of its initial PCE, while the control device can only maintain 67.86% of its initial PCE. Taken together, the ternary solvent system possesses a

positive effect on device stability, which should result from that the ternary solvent system can reduce the surface defects and promote the formation of 2D perovskite capping layer.

3. Conclusion

In summary, a ternary solvent system of passivator was first proposed to maximize the passivation effect of various organic ammonium salts on perovskite surface. This ternary solvent system can not only inhibit the IPA-induced defects during surface passivation, but also promote the penetration of 4-MeO-PEAI and its reaction with perovskite. Owing to the reduced surface defects and sufficient surface passivation, the planar PSCs obtain a PCE of 26.05%. Besides, the unencapsulated devices exhibit excellent long-term stability, which can maintain 95.23% and 95.68% of their initial PCE after 2000 h storage in ambient air and 800 h light-soaking in N_2-glovebox. We believe that this ternary solvent system provides a depth and novel insight into the design of passivator solvent and its influence on passivation effect, assisting the achievement of both high-efficiency single-junction PSCs and tandem PSCs.

Supporting Information

Supporting Information is available from the Wiley Online Library or from the author.

Acknowledgements

Q.Z. and H.H. contributed equally to this work. This work was supported partially by the Key Research and Development Program sponsored by the Ministry of Science and Technology (MOST) (Grant nos. 2022YFB4200301), National Natural Science Foundation of China (Grant nos. 52232008, 51972110, 52102245, 52072121, 52402254 and 22409061), Beijing Natural Science Foundation (2222076, 2222077), Beijing Nova Program (20220484016), Young Elite Scientists Sponsorship Program by CAST (2022QNRC001), 2022 Strategic Research Key Project of Science and Technology Commission of the Ministry of Education, Huaneng Group Headquarters Science and Technology Project (HNKJ20-H88), State Key Laboratory of Alternate Electrical Power System with Renewable Energy Sources (LAPS2024-05), the Fundamental Research Funds for the Central Universities (2022MS029, 2022MS02, 2022MS031, 2023MS042, 2023MS047) and the NCEPU "Double First-Class" Program.

Conflict of Interest

The authors declare no conflict of interest.

Data Availability Statement

The data that support the findings of this study are available from the corresponding author upon reasonable request.

Keywords

high efficiency, perovskite solar cells, solvent, surface passivation

Received: July 17, 2024
Revised: October 7, 2024
Published online:

[1] H. Chen, C. Liu, J. Xu, A. Maxwell, W. Zhou, Y. Yang, Q. Zhou, A. S. R. Bati, H. Wan, Z. Wang, L. Zeng, J. Wang, P. Serles, Y. Liu, S. Teale, Y. Liu, M. I. Saidaminov, M. Li, N. Rolston, S. Hoogland, T. Filleter, M. G. Kanatzidis, B. Chen, Z. Ning, E. H. Sargent, *Science* **2024**, *384*, 189.
[2] B. Ding, Y. Ding, J. Peng, J. Romano-deGea, L. E. K. Frederiksen, H. Kanda, O. A. Syzgantseva, M. A. Syzgantseva, J.-N. Audinot, J. Bour, S. Zhang, T. Wirtz, Z. Fei, P. Doerflinger, N. Shibayama, Y. Niu, S. Hu, S. Zhang, F. F. Tirani, Y. Liu, G.-J. Yang, K. Brooks, L. Hu, S. Kinge, V. Dyakonov, X. Zhang, S. Dai, P. J. Dyson, M. K. Nazeeruddin, *Nature* **2024**, *628*, 299.
[3] NREL, Best Research-Cell Efficiencies, https://www.nrel.gov/pv/cell-efficiency.html, (accessed: October 2024).
[4] S. Tan, T. Huang, I. Yavuz, R. Wang, T. W. Yoon, M. Xu, Q. Xing, K. Park, D.-K. Lee, C.-H. Chen, R. Zheng, T. Yoon, Y. Zhao, H.-C. Wang, D. Meng, J. Xue, Y. J. Song, X. Pan, N.-G. Park, J.-W. Lee, Y. Yang, *Nature* **2022**, *605*, 268.
[5] T. Zhang, F. Wang, H.-B. Kim, I.-W. Choi, C. Wang, E. Cho, R. Konefal, Y. Puttisong, K. Terado, L. Kobera, M. Chen, M. Yang, S. Bai, B. Yang, J. Suo, S.-C. Yang, X. Liu, F. Fu, H. Yoshida, W. M. Chen, J. Brus, V. Coropceanu, A. Hagfeldt, J.-L. Bredas, M. Fahlman, D. S. Kim, Z. Hu, F. Gao, *Science* **2022**, *377*, 495.
[6] H. Huang, P. Cui, Y. Chen, L. Yan, X. Yue, S. Qu, X. Wang, S. Du, B. Liu, Q. Zhang, Z. Lan, Y. Yang, J. Ji, X. Zhao, Y. Li, X. Wang, X. Ding, M. Li, *Joule* **2022**, *6*, 2186.
[7] Q. Feng, G. Nan, *J. Phys. Chem. Lett.* **2022**, *13*, 4831.
[8] Q. Jiang, J. Tong, Y. Xian, R. A. Kerner, S. P. Dunfield, C. Xiao, R. A. Scheidt, D. Kuciauskas, X. Wang, M. P. Hautzinger, R. Tirawat, M. C. Beard, D. P. Fenning, J. J. Berry, B. W. Larson, Y. Yan, K. Zhu, *Nature* **2022**, *611*, 278.
[9] H. Zhang, L. Pfeifer, S. M. Zakeeruddin, J. Chu, M. Gratzel, *Nat. Rev. Chem.* **2023**, *7*, 632.
[10] C. Li, X. Wang, E. Bi, F. Jiang, S. M. Park, Y. Li, L. Chen, Z. Wang, L. Zeng, H. Chen, Y. Liu, C. R. Grice, A. Abudulimu, J. Chung, Y. Xian, T. Zhu, H. Lai, B. Chen, R. J. Ellingson, F. Fu, D. S. Ginger, Z. Song, E. H. Sargent, Y. Yan, *Science* **2023**, *379*, 690.
[11] C. A. R. Perini, E. Rojas-Gatjens, M. Ravello, A.-F. Castro-Mendez, J. Hidalgo, Y. An, S. Kim, B. Lai, R. Li, C. Silva-Acuna, J.-P. Correa-Baena, *Adv. Mater.* **2022**, *34*, 2204726.
[12] T. Wang, Y. Fu, L. Jin, S. Deng, D. Pan, L. Dong, S. Jin, L. Huang, *J. Am. Chem. Soc.* **2020**, *142*, 16254.
[13] J. Zhuang, P. Mao, Y. Luan, X. Yi, Z. Tu, Y. Zhang, Y. Yi, Y. Wei, N. Chen, T. Lin, F. Wang, C. Li, J. Wang, *ACS Energy Lett.* **2019**, *4*, 2913.
[14] Q. Jiang, Y. Zhao, X. Zhang, X. Yang, Y. Chen, Z. Chu, Q. Ye, X. Li, Z. Yin, J. You, *Nat. Photonics* **2019**, *13*, 460.
[15] X. Li, Z. Ying, J. Zheng, X. Wang, Y. Chen, M. Wu, C. Xiao, J. Sun, C. Shou, Z. Yang, Y. Zeng, X. Yang, J. Ye, *Adv. Mater.* **2023**, *35*, 2211962.
[16] S. Tan, T. Huang, I. Yavuz, R. Wang, M. H. Weber, Y. Zhao, M. Abdelsamie, M. E. Liao, H.-C. Wang, K. Huynh, K.-H. Wei, J. Xue, F. Babbe, M. S. Goorsky, J.-W. Lee, C. M. Sutter-Fella, Y. Yang, *J. Am. Chem. Soc.* **2021**, *143*, 6781.
[17] L. Tang, X. Wang, X. Liu, J. Zhang, S. Wang, Y. Zhao, J. Gong, J. Li, X. Xiao, *Adv. Sci.* **2022**, *9*, 2201768.
[18] J. J. Yoo, S. Wieghold, M. C. Sponseller, M. R. Chua, S. N. Bertram, N. T. P. Hartono, J. S. Tresback, E. C. Hansen, J.-P. Correa-Baena, V. Bulovic, T. Buonassisi, S. S. Shin, M. G. Bawendi, *Energy Environ. Sci.* **2019**, *12*, 2192.
[19] F. Wang, W. Geng, Y. Zhou, H.-H. Fang, C.-J. Tong, M. A. Loi, L.-M. Liu, N. Zhao, *Adv. Mater.* **2016**, *28*, 9986.
[20] H. Liu, N. Li, Z. Chen, S. Tao, C. Li, L. Jiang, X. Niu, Q. Chen, F. Wang, Y. Zhang, Z. Huang, T. Song, H. Zhou, *Adv. Mater.* **2022**, *34*, 2204458.
[21] K. M. Muhammed Salim, S. Masi, A. Fabian Gualdron-Reyes, R. S. Sanchez, E. M. Barea, M. Krecmarova, J. F. Sanchez-Royo, I. Mora-Sero, *ACS Energy Lett.* **2021**, *6*, 3511.

[22] Y. Yang, H. Huang, L. Yan, P. Cui, Z. Lan, C. Sun, S. Du, X. Wang, C. Yao, S. Qu, Q. Zhang, M. Wang, X. Zhao, M. Li, *Adv. Energy Mater.* **2024**, *14*, 2400416.
[23] H. Chen, S. Teale, B. Chen, Y. Hou, L. Grater, T. Zhu, K. Bertens, S. M. Park, H. R. Atapattu, Y. Gao, M. Wei, A. K. Johnston, Q. Zhou, K. Xu, D. Yu, C. Han, T. Cui, E. H. Jung, C. Zhou, W. Zhou, A. H. Proppe, S. Hoogland, F. Laquai, T. Filleter, K. R. Graham, Z. Ning, E. H. Sargent, *Nat. Photonics* **2022**, *16*, 352.
[24] B. Yang, J. Suo, F. Di Giacomo, S. Olthof, D. Bogachuk, Y. Kim, X. Sun, L. Wagner, F. Fu, S. M. Zakeeruddin, A. Hinsch, M. Gratzel, A. Di Carlo, A. Hagfeldt, *ACS Energy Lett.* **2021**, *6*, 3916.
[25] R. Azmi, D. S. Utomo, B. Vishal, S. Zhumagali, P. Dally, A. M. Risqi, A. Prasetio, E. Ugur, F. Cao, I. F. Imran, A. A. Said, A. R. Pininti, A. S. Subbiah, E. Aydin, C. Xiao, S. I. Seok, S. De Wolf, *Nature* **2024**, *628*, 93.
[26] S. Ramakrishnan, D. Song, Y. Xu, X. Zhang, G. Aksoy, M. Cotlet, M. Li, Y. Zhang, Q. Yu, *Adv. Energy Mater.* **2023**, *13*, 2302240.
[27] L. Chen, C. Li, Y. Xian, S. Fu, A. Abudulimu, D.-B. Li, J. D. Friedl, Y. Li, S. Neupane, M. S. Tumusange, N. Sun, X. Wang, R. J. Ellingson, M. J. Heben, N. J. Podraza, Z. Song, Y. Yan, *Adv. Energy Mater.* **2023**, *13*, 2301218.
[28] L. Liu, C. Zheng, Z. Xu, Y. Li, Y. Cao, T. Yang, H. Zhang, Q. Wang, Z. Liu, N. Yuan, J. Ding, D. Wang, S. Liu, *Adv. Energy Mater.* **2023**, *13*, 2300610.
[29] L. Yan, H. Huang, P. Cui, S. Du, Z. Lan, Y. Yang, S. Qu, X. Wang, Q. Zhang, B. Liu, X. Yue, X. Zhao, Y. Li, H. Li, J. Ji, M. Li, *Nat. Energy* **2023**, *8*, 1158.
[30] X. Yue, Y. Yang, X. Zhao, B. Fan, H. Yan, S. Qu, Q. Zhang, Z. Lan, S. Du, H. Huang, L. Yan, X. Wang, P. Cui, J. Ma, M. Li, *Phys. Chem. Chem. Phys.* **2023**, *25*, 9349.
[31] X. Wang, H. Huang, M. Wang, Z. Lan, P. Cui, S. Du, Y. Yang, L. Yan, Q. Zhang, S. Qu, M. Li, *Adv. Mater.* **2024**, *36*, 2310710.
[32] N. Yan, Y. Gao, J. Yang, Z. Fang, J. Feng, X. Wu, T. Chen, S. Liu, *Angew. Chem., Int. Ed.* **2023**, *62*, 202216668.